

# The Journal of Undergraduate Research in Physics

## CONTENTS

ANALYSIS OF ELECTRON-ATOM COLLISIONS IN  
MERCURY VAPOR BY PHOTON EMISSION.....29

Steven R. Cain  
Connecticut College  
New London, CT

MONTE CARLO CALCULATIONS OF THE BACKGROUND OF  
SINGLE PHOTONS PRODUCED BY THE DECAY OF A  
PION IN THE R808 EXPERIMENT AT CERN.....35

Merritt Jacob  
University of Pittsburgh  
Pittsburgh, PA

OBSERVATION OF RESISTIVITY ENHANCEMENT IN  
ULTRA-THIN SILVER FILMS.....41

David R. Fazzini, Franklin E. Baumann and  
Phillip D. Radusewicz  
Illinois Institute of Technology  
Chicago, IL

VOLUME 5, NUMBER 2

WINTER 1987

Published by Guilford College  
for

The American Institute of Physics and The Society of Physics Students



## THE JOURNAL OF UNDERGRADUATE RESEARCH IN PHYSICS

This journal is devoted to research work done by undergraduate students in physics and its related fields. It is to be a vehicle for the exchange of ideas and information by undergraduate students. Information for students wishing to submit manuscripts for possible inclusion in the Journal follows.

### ELIGIBILITY

The author must have performed all work reported in the paper as an undergraduate. The subject matter of the paper is open to any area of pure or applied physics or physics related field.

### SPONSORSHIP

Each paper must be sponsored by a full-time faculty member of the department in which the research was done. A letter from the sponsor to the editor must accompany the manuscript if it is to be considered for publication.

### FORM

The manuscript should be typed, double spaced, on 8 1/2 x 11 inch sheets. Margins of about 1 1/2 inch should be left on the top, sides, and bottom of each page. Papers should be limited to twelve pages of text in addition to an abstract and appropriate drawings, pictures, and tables.

### GENERAL STYLE

All papers must conform to the Style Manual of the American Institute of Physics. Each paper must be prefaced by an abstract that does not exceed 250 words.

### ILLUSTRATIONS

Line drawings should be made with black India ink on plain white paper. If a graph is drawn on co-ordinate paper, the paper must be lined blue. Important lines should be ruled in black. Each figure or table must be on a separate sheet. Photographs must have a high gloss finish.

### CAPTIONS

A brief caption should be provided for each illustration or table, but it should not be part of the figure. They should be listed together at the end of the manuscript.

### EQUATIONS

Equations should appear on separate lines and may be written in black India ink.

### FOOTNOTES

Footnotes should be typed double spaced and grouped together in sequence at the end of the manuscript.

### SUBMISSION

Two copies of the manuscript and a letter from the sponsor should be sent to:  
Dr. Rexford E. Adelberger, Editor  
THE JOURNAL OF UNDERGRADUATE RESEARCH IN PHYSICS  
Physics Department  
Guilford College  
Greensboro, NC 27410

### SUBSCRIPTION INFORMATION

The Journal will be published biannually with issues appearing in Summer and Winter of each year. There will be two issues per volume.

| TYPE OF SUBSCRIBER | PRICE PER VOLUME |
|--------------------|------------------|
| Individual         | \$ 5.00          |
| Institution        | \$10.00          |

Foreign subscribers add \$2.00 for surface postage, \$10.00 for air postage.

To receive a subscription, send your name, address, and check made out to The Journal of Undergraduate Research in Physics (JURP) to:

Journal of Undergraduate Research in Physics  
Physics Department  
Guilford College  
Greensboro, NC 27410

### BACK ISSUES

Back issues may be purchased by sending \$10.00 per volume to the editorial office.

ISSN 0731 - 3764

The Journal of Undergraduate Research in Physics is published by Guilford College for the American Institute of Physics and the Society of Physics Students.

## AN EDITORIAL

The Journal is looking forward to publishing book reviews written by student readers of the Journal. Any member of the Society of Physics Students can submit a review of a text book that the individual has used in a course. We feel that this will provide a needed and useful service to faculty who are trying to decide which text to use.

The following is a set of guidelines for book reviewers:

## A. Mechanical Details

1. Keep the length between 250 and 400 words.
2. Submit two copies, typed and double spaced to the Editorial Office:  
JURP  
Physics Department  
Guilford College  
Greensboro, NC 27410
3. Include a title for your review.
4. Be sure to indicate your name, the school you attend including the address and ZIP code.
5. Tell what course and at what level (junior etc.) the text you are reviewing was used.

## B. Contents of the review.

1. Give a summary of the content of the text, but try to avoid an item by item listing of topics.

2. Evaluate the quality of the text in terms of a) subject content, b) accuracy, c) depth, d) homework problems and worked examples and e) the level and excellence of the writing style.

3. Was this text helpful in your understanding of the subject material? Would you choose this text if you were to teach the course next year? Why?

4. An overall evaluation of the book as a text is much more valuable than a listing of faults, misprints, etc. Flaws should be cited, however, if they are indicative of what you find to be the general quality of the book.

5. Was the text presented in such a manner that it was easy to use? Is the table of contents well organized? Are the appendices useful?

6. What would you change if you were the editor of the next edition of the text?

Please consider writing a review of one of the texts you used this year. The experience will be good for you and you may help a faculty member choose a better text for a similar course taught in the future.

## ANALYSIS OF ELECTRON-ATOM COLLISIONS IN MERCURY VAPOR BY PHOTON EMISSION

Steven R. Cain  
 Department of Physics and Astronomy  
 Connecticut College  
 New London, CT 06320

## ABSTRACT

This experiment investigates the optical transitions that occur as a result of electron-atom collisions in a mercury vapor. A number of the transitions were identified. We found that the number of photons produced was dependent upon the number of electrons available for collisions. The intensity of photons rose as the energy increased, reached a maximum and then fell off. The intensity for a particular transition decreased as the principle quantum number of the upper level increased.

## INTRODUCTION

This experiment is an investigation of electron-atom collisions within mercury vapor. We observed and identified optical transitions occurring as a result of the collisions between the electron and the atom. We also studied the effect that electron energy and the number of electrons available for collisions have on the intensity of the emitted light.

Mercury is a difficult substance with which to work because it condenses easily at standard conditions. Mercury depositions can contaminate experimental apparatus and are difficult to clean. As a consequence, relatively little work has been done with the atom under these conditions (1). The most extensive work was done by Jorgenus (2).

In the present work, the problem of mercury depositions was avoided by the use of an electron tube. These tubes are inexpensive and easily procurable (3). They are entirely self-contained, so the acceleration and collisions occur within the tube.

## EXPERIMENTAL PROCEDURE

The apparatus used to identify the transitions consisted of a mercury vapor electron tube with a tungsten filament cathode and a cylindrical anode. Two power supplies were used, one as a current source for the

filament and the other to supply the potential between the electrodes. Light emitted from the collisions was then analyzed using a spectrometer which separated the light into its component wavelengths. The spectrometer was calibrated using the spectrum of hydrogen as a standard.

Once the wavelengths of the transitions were measured, additions were made to the apparatus to measure the intensities of some of the spectral lines of mercury (see Figure 1). A circular, double convex lens was inserted between the tube and the

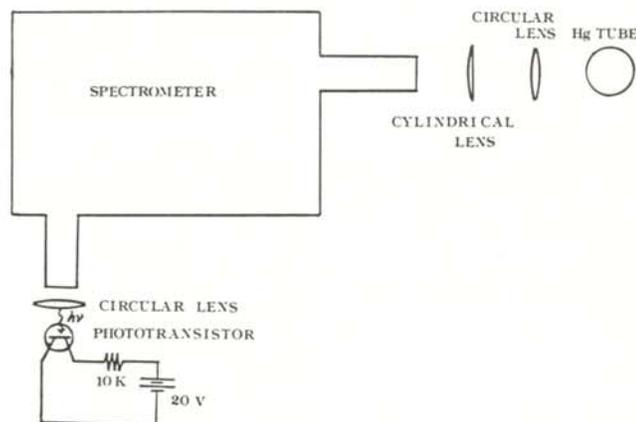


Figure 1  
 Schematic diagram of the apparatus and photo-transistor circuit.

spectrometer to produce a beam of parallel light. Then a cylindrical, plano-convex lens was used to focus the parallel light down to a line on the entrance slit of the spectrometer. At the other end of the spectrometer, another circular, double convex lens was used to focus the emerging light onto a photo-transistor (4).

This photo-transistor was part of a simple circuit used to measure the intensities of the different spectral lines. This circuit, also shown in Figure 1, was composed of the transistor, a 10 KOhm resistor at its collector, and a power supply which maintained a bias voltage of 20 V between the collector and emitter. The intensity of the light was obtained by measuring the voltage drop across the resistor.

This voltage is proportional to the current flowing through the resistor, which, in this case, is also the collector current of the transistor. The collector current is proportional to the intensity of the light as shown in the following equation:

$$I(c) = (h(fe) + 1)LR \quad (1)$$

where  $I(c)$  is the collector current,  $h(fe)+1$  is the gain of the transistor,  $L$  is the intensity of the light, and  $R$  is the response of the transistor to the wavelength (5). Thus, the voltage across the resistor is proportional to the intensity of the light incident on the base of the transistor.

TABLE 1

| Wavelength: (angstroms)  | transitions         |
|--------------------------|---------------------|
| 6234                     | $9p^3P - 7s^2S_0$   |
| 6150*                    |                     |
| 6072 (6072.713, 6072.72) | NOT IDENTIFIED      |
| 5791: 5789.66            | $6d^3D_2 - 6p^1P_2$ |
| 5790.66                  | $6d^1D_2 - 6p^2P_2$ |
| 5790.663                 | NOT IDENTIFIED      |
| 5770                     | $6d^3D_2 - 6p^3P_1$ |
| 5461                     | $7s^3S_2 - 6p^3P_2$ |
| 4917                     | $8s^2S_0 - 6p^3P_2$ |
| 4358                     | $7s^3S_2 - 6p^3P_2$ |
| 4339                     | $7d^3D_2 - 6p^2P_2$ |

\*This line is apparently not a mercury line. The most probable source is tungsten.

The response of the optical system as a function of wavelength was measured over the interval from 3900 to 6700 Angstroms. This was done by comparing the known calibration curve of a tungsten lamp to the observed intensity distribution. From this data, a correction function for intensity versus voltage across the resistor for the transistor was obtained. With this correction function, the voltage across the resistor was manipulated into intensity values for the various emitted wavelengths

Measurements of the intensity of the emitted light and the current between the electrodes were made at three different filament currents: 1.6 A, 1.8 A, and 2.0 A. At each of these currents, the accelerating potential was varied to observe how the number of electrons present (anode current) and electron energy (accelerating potential) affected the intensity of a particular transition.

#### DISCUSSION OF RESULTS

Table 1 shows the wavelengths and corresponding transitions observed (6). How the intensity of five of these varied as the filament current and the potential between the electrodes were varied was measured. Some of these results are shown in Figure 2.

For each of the wavelengths observed, large increases in intensity occurred just after (within 6 Volts) the first and second ionization potentials of mercury (7). Accompanying these increases was a "clouding" of the tube with light. It is doubtful that this clouding can be explained simply by the scattering of the incident electrons producing secondary collisions. At these energies, the differential scattering cross section of mercury decreases sharply as the angle of deflection increases from zero (8). A more satisfactory explanation is that the incident electrons were ionizing the mercury atoms and that the ejected electrons were scattering randomly throughout the tube. The fact that the clouding of the tube occurred just above the ionization potentials of the atom would seem to justify this explanation.

However, the analysis of the spectrum did not provide any evidence that ionization was occurring as all

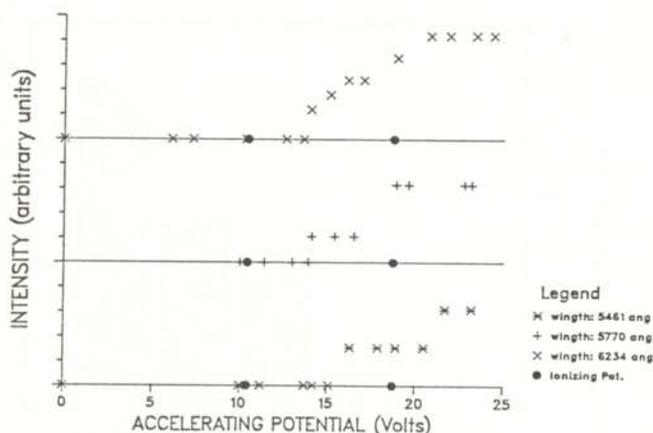


Figure 2  
These curves show the large increases in the intensity occurring shortly after the accelerating potential is above the ionizing potentials of the mercury atom.

the lines we found were from the neutral atoms. This is not surprising because at these collisional energies, there would be little excess energy above the ionization potential that could be used in excitation. Recombination was probably occurring quite rapidly, reducing the number of mercury ions present.

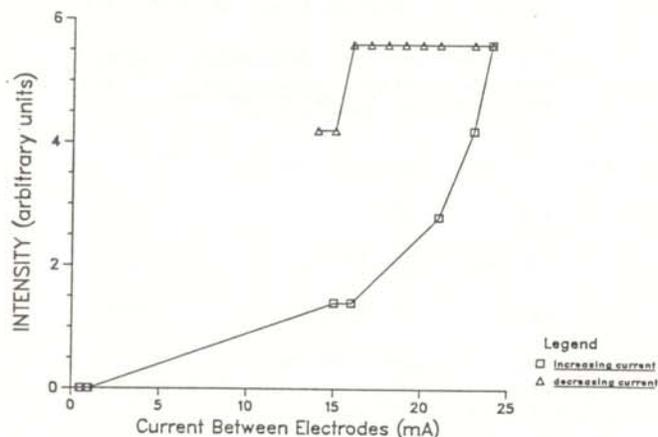


Figure 3  
This curve shows the non-linear behavior of the current between the electrodes and the intensity of the emitted light.

Further evidence that ionization was occurring and that these ejected electrons were a major source of excitation was found in the data relating the current flow between the electrodes and the intensity. If the electrons from the filament were the only source of electrons for collisions, then the intensity would be proportional to the current flowing between the electrodes. However, the

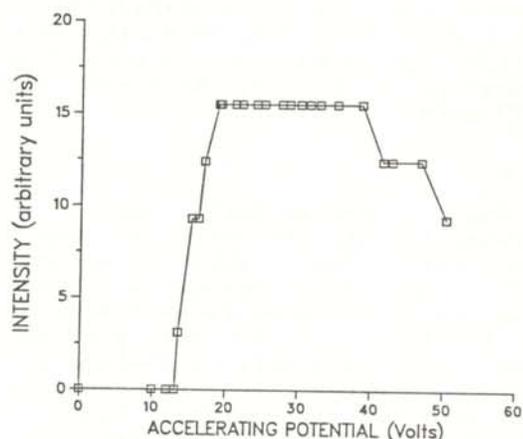


Figure 4  
The intensity of the light as a function of the accelerating potential. The uncertainty of the measurements is about 20%.

data showed (see Figure 3) that this was not the case. The intensity rose with the current, but as the current began to fall off, the intensity fell off at a markedly slower rate. It was also observed that when the intensity of the light was saturated, the filament current source could be completely turned off and the intensity would not fall off. This shows that electron-atom collisions were occurring even though there was no outside current source. The only other source of electrons was the mercury atoms themselves. Thus, a self-sustaining plasma was produced.

The data relating the intensity to accelerating potential showed that as the potential increased, the intensity rose to a maximum and then began to fall off (see Figure 4). This is in

qualitative agreement with the finding of Jorgenius and others (9). Their data showed that the excitation functions of mercury followed similar curves.

The relative intensity of the different lines also support the findings of Semenova and Smirnov (1) which show that the intensity of the light decreases as the principle quantum number of the upper level increases (see Figure 5). There is an apparent discrepancy in our data. Two 7S-6P transitions (4358 and 5461 Angstroms) had a higher maximum intensity than the 6D-6P transition (5771 Angstroms). This is explained by the fact than in the mercury atom, the 6D level is actually higher energy than the 7S level (10).

#### CONCLUSION

The data showed that large increases in intensity occurred when the mercury was ionized. This caused the number of electrons present to produce collisions to increase dramatically. Thus, the intensity was greatly affected by the number of electrons available to produce collisions. However, the same is not true for the energy of the electrons. Our data showed that, although it does affect the intensity of light emitted, its affect is not nearly as pronounced as that of the number of electrons present. The intensity of an individual spectral line is dependent upon the energy level from which the transition originates.

#### REFERENCES

- (1) I.V. Semenov, Y.M. Smirnov, *Optics and Spect.*, 42 477 (1977), and N.P. Penkin, T.P. Redko, *Optics and Spect.*, 36 258 (1974).
- (2) H. Massey., E. Burhop, H. Gilbody, *Electronic and Ionic Impact Phenomena, Vol I*, Oxford University Press, Oxford, 1969, pp. 216-222.
- (3) Type 866 mercury vapor tube, manufactured by RCA, available from Newark Electronics, Chicago, IL.
- (4) Photo-transistor ECG3036 available from Newark Electronics, Chicago, IL.

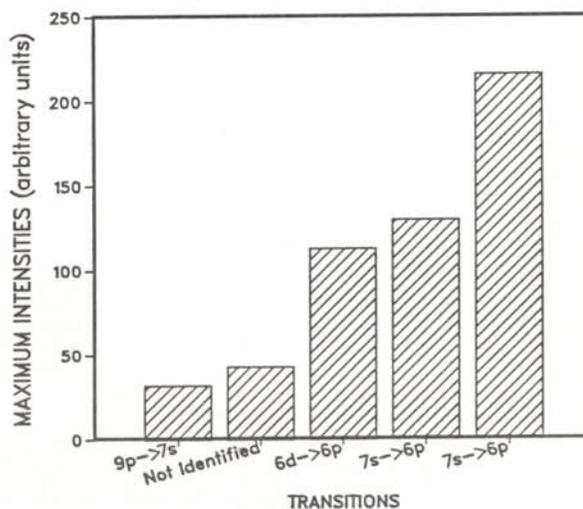


Figure 5  
The intensity of a particular transition as a function of the principle quantum number of the upper level.

- (5) A.J. Diefenderfer, *Principles of Electronic Instrumentation*, Saunders Publishing, Philadelphia, 1979, p. 399.
- (6) Massey, *op.cit.* p. 218, and J. Reader, C.H. Corliss, *Wavelengths and Transition Probabilities for Atoms and Atomic Ions*, National Bureau of Standards, NSRDS, 1980.
- (7) R.F. Bacher, S. Goudsmit, *Atomic Energy States*, McGraw-Hill, New York, 1932, pp.277,231.
- (8) Massey, *op.cit.* pp.332-339.
- (9) *Ibid.* p.219.
- (10) Bacher, *op.cit.* pp. 227-228.

#### FACULTY SPONSOR OF THIS PAPER

Professor Michael Monce  
Department of Physics and Astronomy  
Connecticut College  
New London, CT 06320

MONTE CARLO CALCULATIONS OF THE BACKGROUND OF SINGLE PHOTONS PRODUCED BY THE  
DECAY OF A PION IN THE R808 EXPERIMENT AT CERN

Merritt Jacob  
Department of Physics and Astronomy  
University of Pittsburgh  
Pittsburgh, PA 15260

ABSTRACT

Monte Carlo data and simulations were used to predict the ratio of apparent direct photons to pions in the axial field spectrometer located at the CERN intersecting storage rings. The detection of two photons with the proper spatial separation and energies to form an invariant mass consistent with that of the pion can be used to indicate the presence of a pion. All other photons detected were said to be direct photons. However, some times only one of the two photons of the pion decay could be detected. An algorithm was developed to predict these events, providing a way of separating out the true number of pions from the direct photon data.

INTRODUCTION

The intersecting storage rings (ISR) at CERN are two colliding beams of protons of momentum 61.5 GeV/c. This provides a proton-proton collision with a center-of-mass energy of 63 GeV (1). One of the goals of the R808 experiment at the ISR was to determine the gluon distribution in a proton via the detection of direct photons at high transverse momentum produced in proton-proton interactions (2). The reactions that produce direct photons are:

Quark Quark  $\rightarrow \gamma + \text{other stuff}$   
Gluon Quark  $\rightarrow \gamma + \text{other stuff}$

The second reaction is known as the Quantum Chromodynamic Compton effect (3). In this experiment we studied the direct photons which were produced and then inferred the properties of the quarks or the distribution in momentum fraction of the gluon in the proton.

The detectors used in this experiment consisted of an inner hodoscope, which is an array of scintillators used to detect two or more charged particles, a cylindrical drift chamber and a 2  $\pi$  uranium/copper scintillator calorimeter. The photon detector was constructed of sodium iodide crystals, optically separated

into 20 x 30 arrays on opposite sides of the detector. The assembled hybrid detector is shown in Figure 1. Figure 2 shows the side view and Figure 3 shows the top view of the path of a typical photon jet event inside the detector.

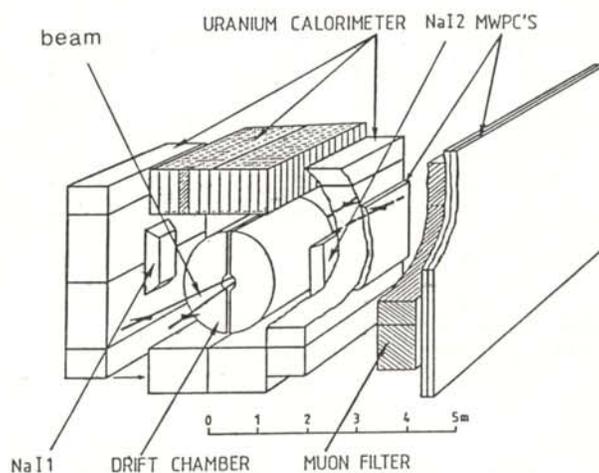


Figure 1  
Schematic diagram of the detector. The two NaI crystal walls are made up of 20x30 arrays of individual crystals.

Single photons, other than those produced directly, could be detected by the counter. The major contributor to this background was the decay of the neutral pion into two photons where only one photon was seen because the other was outside the detector or its energy was too small to be detected in the NaI crystals, or the photons were so close together that they appeared to be "merged" as a single photon.

In this paper we discuss the calculation of the background caused merged events. The Monte Carlo (4) predictions about the merging were done by us and at CERN with different results. This discrepancy was resolved

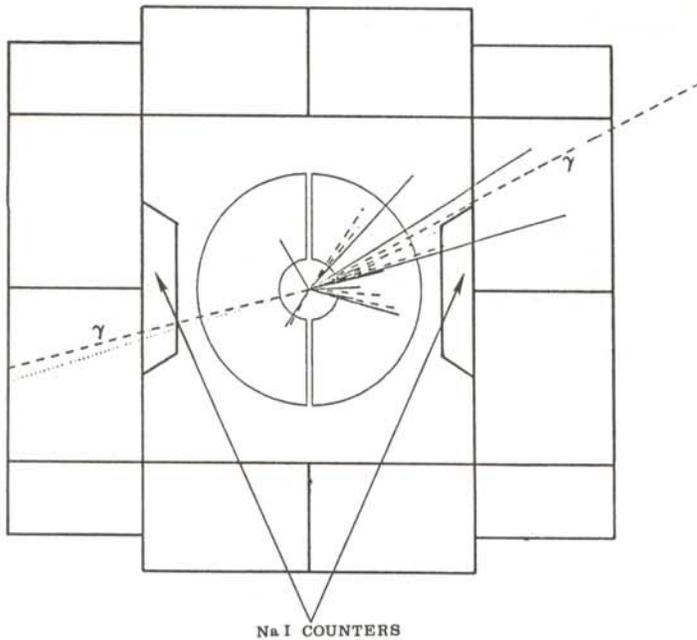


Figure 2  
Side view of a typical photon jet event inside the detector.

by modifying the CERN Monte Carlo data threshold.

THE MONTE CARLO SIMULATION

To investigate the merging problem, Monte Carlo "EGS" (Electromagnetically generated showers) (5) data were created at CERN and later

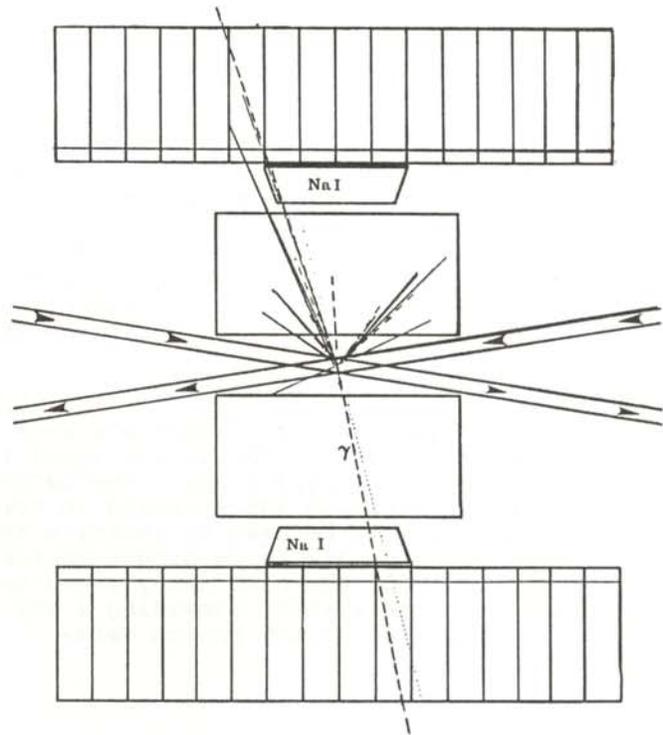


Figure 3  
Top view of a typical photon jet event inside the detector.

transported to the University of Pittsburgh and studied. The Monte Carlo simulation consisted of a program which gave the reconstruction efficiencies, the probability of the two photons being reconstructed as a pion (6), of the  $\gamma$  and  $\pi^0$  as a function of photon separation and lab energy. These efficiencies were then fitted, unaided by a computer, with functions and incorporated into another program which produced the  $\gamma$  to  $\pi$  background ratio. A summary of this work is shown in Figure 4.

The photon to pion background curves generated by the program are shown in Figures 5 and 6. The calculations are shown with the data from the experiment. One can clearly see that the background is less than the data. This was not true of the data generated by the simulation developed at CERN. Using these results and the and efficiencies, the corrected gamma to pi ratio was calculated using:

$$\gamma/\pi^0(\text{corrected}) = (\gamma/\pi^0(\text{data}) - \gamma/\pi^0(\text{background})) * \pi^0 \text{ efficiency} / \gamma \text{ efficiency}$$

|                                       | WALL 1                            |                                   | WALL 2                            |
|---------------------------------------|-----------------------------------|-----------------------------------|-----------------------------------|
|                                       | R <sub>CUT</sub> = 20 cm          | R <sub>CUT</sub> = 25 cm          | R <sub>CUT</sub> = 20 cm          |
| $\epsilon_{\pi}(E_{\pi})$             | $.66(1 - e^{-(E_{\pi}-3.4)/2.5})$ | $.66(1 - e^{-(E_{\pi}-3.4)/2.5})$ | $.66(1 - e^{-(E_{\pi}-3.8)/3.0})$ |
| $\epsilon_{\pi}(\gamma-\gamma_{sep})$ | $\epsilon_{\pi}(E_{\pi}) * \eta$  | $\epsilon_{\pi}(E_{\pi}) * \eta$  | $\epsilon_{\pi}(E_{\pi}) * \eta$  |
| $\epsilon_{\gamma}(E_{\gamma})$       | $.60(1 - e^{-(E-3.4)/4.7})$       | $.70(1 - e^{-(E-3.3)/4.7})$       | $.60(1 - e^{-(E-3.9)/5.7})$       |
| $\gamma/\pi(\gamma-\gamma)$           | $.01 + .05(4.1 - \gamma_{sep})$   | $.02 + .08(5 - \gamma_{sep})$     | $.01 + .05(4.1 - \gamma_{sep})$   |

Figure 4  
 efficiency of the pion reconstructions as a function of either the pion energy ( $E_{\pi}$ ) or of the separation of the photons detected ( $\gamma \gamma_{sep}$ ).  $\epsilon_{\gamma}$  is the efficiency of single photon detection as a function of the energy of the photon.  $\gamma_{sep}$  is the ratio of gammas to pions as a function of photon separation.  $\eta$  is a scaling correction factor for the fit.  $R_{cut}$  is the radius of the photon energy distribution in the NaI walls of the detector.

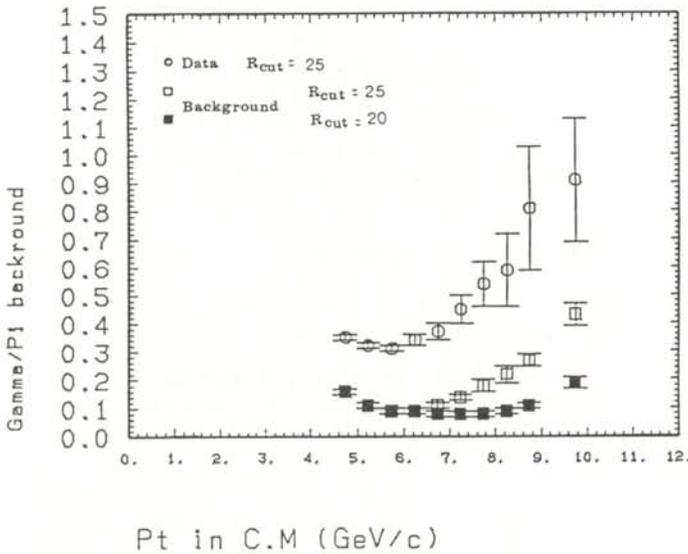


Figure 5  
 Gamma/Pi background for Wall I, comparing the data and simulations with different cuts.

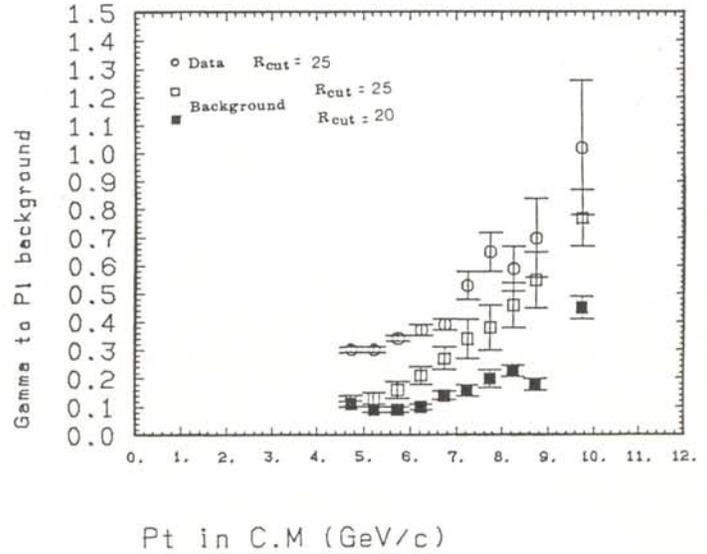


Figure 6  
 Gamma/Pi background for Wall II, comparing the data with simulated values.

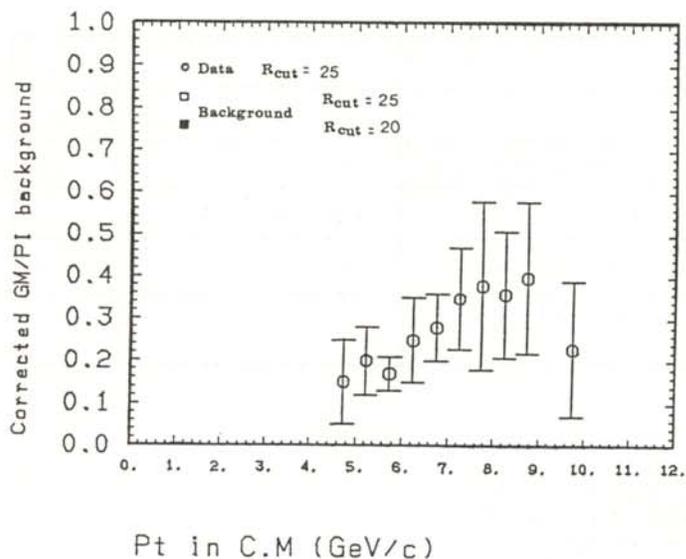


Figure 8  
Corrected Gamma/Pi background for Wall II. Comparison with Figure 6 shows that it is certainly less than the data.

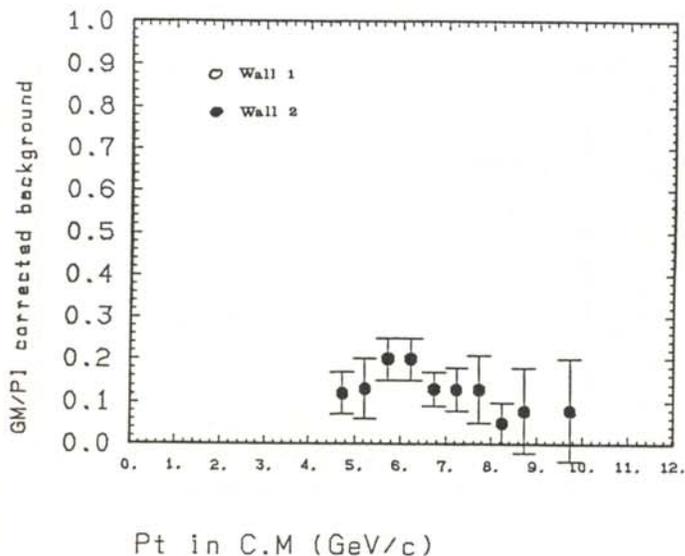


Figure 7  
Corrected Gamma/Pi background for Wall I. Comparison with Figure 5 shows that it is certainly less than the data.

The corrected ratios are shown in Figures 7 and 8. The corrected backgrounds for each wall of detectors are compared in Figure 9. There is good agreement up to about 6 GeV/c. Because of the center of mass motion towards wall II, caused by the beams intersecting at a slight angle, 6 GeV/c of transverse momentum in the center of mass frame in wall II corresponds to about 7 GeV/c in the lab frame. Thus, we seem to begin having consistency problems around 7 GeV/c in the lab frame. This corresponds to 8 GeV/c in the center of mass frame for wall I. Thus, we trust the wall II values up to 6 GeV/c and the wall I values up to around 8 GeV/c.

DISCUSSION OF CERN RESULTS

While our Monte Carlo simulation

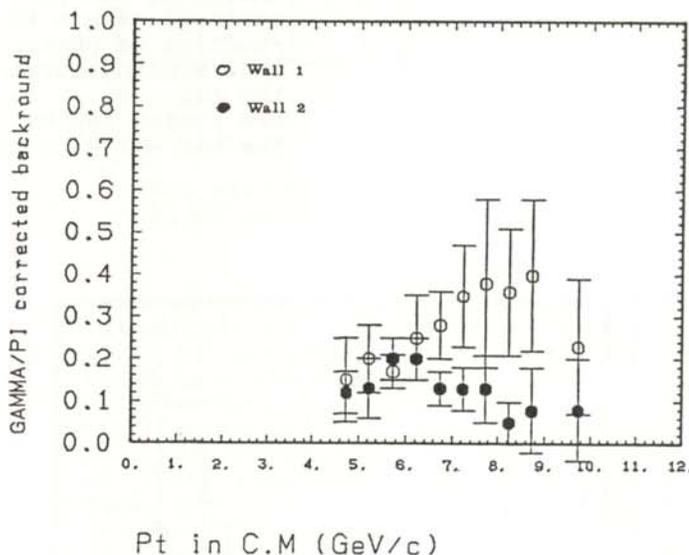


Figure 9  
Comparison of the corrected background for the two walls. There is good agreement until about 6 GeV/c.

produced a background which was lower than the data (with some wall disagreement), that done at CERN did not. We believe that this is due to some procedural differences. Some were of little quantitative consequences, such as error handling. The most prominent serious problem was the type

of functions used to fit the different efficiencies. CERN used computer generated error functions (the integral of a Gaussian) We used the best possible fit to a linear, spline, or quadratic functions. The error functions are not inconsistent with the Monte Carlo "data" points, but they are flatter at higher energies than those we used. We view the difference between the two fits as indicative of systematic errors in the fitting procedure.

The discrepancy between the results for the two walls may be handled by comparing the data with the simulation and comparing the results for the two walls. In this manner one can infer how much to adjust the background as a function of energy in the lab frame.

The cause of the rise in the background gamma to pi ratio is merging photons from the neutral pion decay that the detector sees as single direct photon. The discrepancy between the results for the two walls of detectors is even more severe in the CERN results. We believe that it is due to a quirk in the reconstruction program, coupled with slightly more prominent shower distribution tails in the data than in the Monte Carlo simulation.

The program looks at a three by three NaI crystal area and decides if the energy deposited is correct for a single photon. If the ideal single photon distribution is similar to the one in Figure 10a, it is possible that two merged photons may appear to the detection program as a single photon if no energy is detected outside the 3 x 3 array of crystals (see Figure 10b).

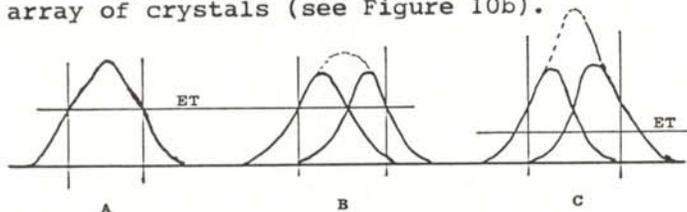


Figure 10

The effect of the tail on the detection of merged photons. Figure 10a is an ideal single direct photon. Figure 10b shows two merged photons that because of the high energy threshold appear to be one. If the energy threshold is lowered as in Figure 10c, the sum has too large an energy to be a single photon.

However, if the energy threshold is lowered, the tails of the photons become visible. The reconstruction program might then recognize this as two separate photons (see Figure 10c).

In the data, the tails were relatively more prominent and were recognized by the reconstruction program as two separate photons. Because these tails were not seen in the Monte Carlo simulation, the two merged photons were more often interpreted as a single direct photon, thus raising the background ratio. This factor, along with the unfortunate fits of the efficiencies, were enough to raise the CERN gamma to pi background above the data. This theory about the cause of the problems with the merging photons was tested at CERN by lowering the threshold in processing the Monte Carlo data. The merging problem was found to be gone.

#### ACKNOWLEDGMENTS

The author gratefully acknowledges the work of all the people who developed and took the data for R808 at CERN. He especially wants to recognize H. Breuker, V. Goerlack and R. Kroeger.

#### REFERENCES

- (1) M.G. Alabrow, C.W. Fabjan and M. Jacob, Editors, Selected Topics in ISR Physics, CERN 82-11 Experimental Physics Division, 15 Nov., 1982.
- (2) T. Akesson, et.al. Phys. Scr. **23**, 649 (1981).
- (3) T. Ferbell and W.R. Molzon, Reviews of Modern Physics, **56**, 181, (1984).
- (4) M.H. Kalso and P. A. Whitlock, Monte Carlo Methods Vol 1: Basics, John Wiley & Sons, 1986.
- (5) R.L. Ford and W.R. Nelson, SLAC-210 (1978).
- (6) T. Akesson, et.al., Phys. Lett., **158B**, 282, (1985).

#### FACULTY SPONSOR OF THIS PAPER

Dr. Julia A. Thompson  
Department of Physics and Astronomy  
University of Pittsburgh  
Pittsburgh, PA 15260

## OBSERVATION OF RESISTIVITY ENHANCEMENT IN ULTRA-THIN SILVER FILMS \*

David R. Fazzini, Franklin E. Baumann and Phillip D. Radusewicz  
 Physics Department  
 Illinois Institute of Technology  
 Chicago, IL 60616

## ABSTRACT

It has been observed that the electrical resistivity of ultra-thin silver films is no longer an intrinsic property when the film thickness is decreased below the electron mean-free-path of silver. We measured the resistivity of silver films with thicknesses ranging from about 160 nm to about 7.5 nm and found that the resistivity increased by a factor of up to 25 for our thinnest films. These results do not fit the theoretical model of resistivity in thin films as reviewed by Campbell (L.I. Maissel, Handbook of Thin Film Technology, McGraw-Hill, New York, 1970). We postulate that this inconsistency arises from the onset of island nucleation which is not considered in the model.

## INTRODUCTION

Electrical resistivity is generally considered an intrinsic property of a metal. It only has to do with the type of metal in question and not with the dimensions of the metal. The resistivity,  $\rho$ , of a metal is defined as the ratio of the electric field intensity  $E$  to the current density  $J$ :

$$\bar{E} = \rho \bar{J} \quad (1)$$

This can be shown to be (1):

$$\rho = \frac{m V_r}{N e^2 \lambda} \quad (2)$$

where  $m$  is the effective electron mass,  $N$  is the number of conduction electrons per volume,  $e$  the electronic charge,  $V_r$  the random velocity of the electrons, and  $\lambda$  the mean-free-path for electrons in the material.

Equation 2 indicates that the resistivity depends inversely upon the electron mean-free-path. Since the mean-free-path is the average distance traveled by an electron between two successive collisions, it is not clear how the resistivity behaves if one of the dimensions of the metal were made smaller than the value of  $\lambda$ . This

experiment is an attempt to determine this behavior.

## EXPERIMENTAL PROCEDURE

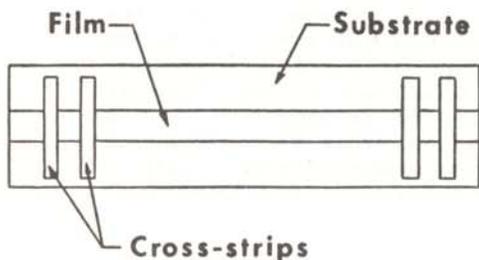
In order to measure the resistivity of a metal sample with one dimension smaller than the mean-free-path for electrons, we evaporated thin films of silver onto glass substrates. The films were made with a variety of thicknesses.

The first step in the experiment was the preparation of sufficiently clean glass slide substrates. Ordinary glass slides were washed in detergent and water, and then rinsed with acetone to remove any contaminants that could affect film adhesion and the electrical properties of the thin sample. Care was taken not to wipe the slide surface with any type of cloth to insure a smooth surface for film deposition.

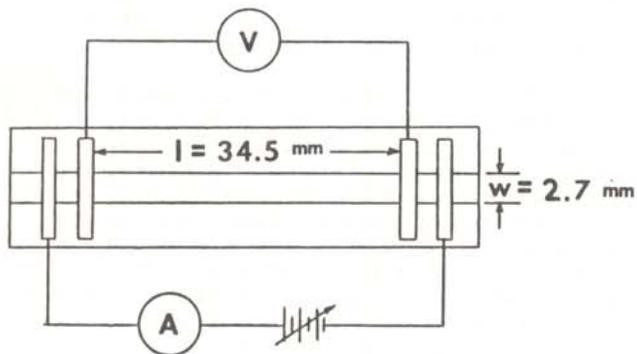
The substrates were then positioned within a holder inside a vacuum chamber. The system was evacuated by means of a mechanical roughing pump and a diffusion pump to a pressure of  $5 \times 10^{-5}$  Torr. A piece of high purity silver, placed in a tantalum (Ta) foil boat, was placed inside the vacuum chamber. The silver was raised above its melting point by the Ohmic heating of the boat. This leads to the evaporation of the silver which deposits onto the clean glass

slide. The deposition took place at a rate of about 0.3 nm per second. The rate was controlled by the current passing through the Ta boat and measured by the frequency change of a quartz monitor placed near the substrate.

The silver was deposited onto the substrate in a manner that allowed four-terminal resistance measurements to be made. This was accomplished by using two masks. The first made a narrow strip lengthwise across the



(a)



$$R = \frac{V}{I}$$

$$\rho = \frac{Rwd}{l}$$

(b)

Figure 1  
A typical silver film preparation (a), and the same film in a four-terminal configuration (b).

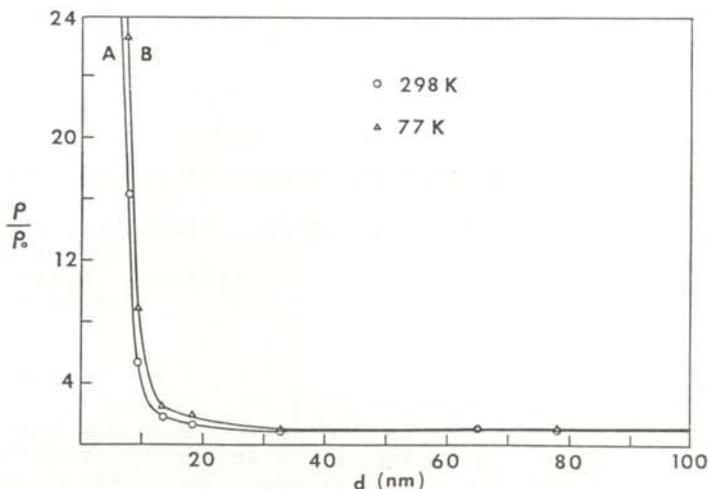


Figure 2  
Ratio of the film resistivity to the bulk resistivity as a function of film thickness. Curve A represents the data at 298K. Curve B is the data at 77K. The evaporation rate for producing this film was .3 nm/sec.

substrate. This was the film from which the electrical measurements were made. The second mask was used to make four cross-strips, perpendicular to the narrow strip mentioned above. A schematic diagram of a typical film is shown in Figure 1. Four wire leads were attached to the cross-strips with indium solder.

Nine silver films, ranging in thickness from about 7.5 nm to about 160 nm were fabricated in this manner. The average resistivity for each film was computed from several current voltage measurements. All resistivity measurements were initially done at 298K and then repeated at 77K by immersing the films directly into liquid nitrogen.

RESULTS AND DISCUSSION

The behavior of resistivity as a function of film thickness is shown in Figure 2 for temperatures of 298K and 77K. To understand this behavior, one first must understand the concept of resistivity. Loosely bound conduction electrons in a metal give rise to electrical conductivity. The scattering of these electrons by the rest of the metal produces resistivity. In clean films, the electrons are

primarily scattered by lattice vibrations (phonons), causing a temperature dependent electron mean-free-path ( $\lambda$ ). Comparison of the resistivity of our thickest films with the handbook values for clean silver (2), we obtained an estimate for  $\lambda$  of 36.5 nm at room temperature.

Figure 2 shows that the resistivity starts to increase gradually near our estimated mean-free-path. At 298K, we note that the resistivity is twice the bulk resistivity when the film thickness is about half of the mean-free-path. Equation 2 suggests that the film thickness actually becomes the effective electron mean-free-path. At 77K, the resistivity starts to increase at a smaller thickness than at room temperature. This is expected since at lower temperatures there is less electron scattering due to phonons.

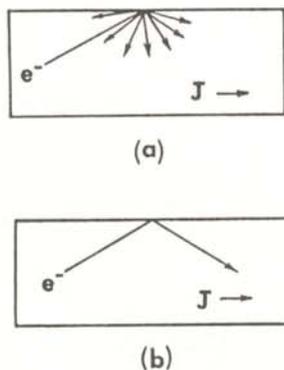


Figure 3  
Diffuse (a) and specular (b) scattering. In diffuse scattering, the electron has an equal probability of being scattered in any direction after its collision with the surface. In specular scattering, the electron scatters in a manner such that it does not change the current density from what would be expected for the bulk material.

Figure 2 also shows a very dramatic increase in resistivity when the film thickness is decreased below a critical value. From our data, we estimate this critical thickness to be about 10 nm. To understand the

behavior of the resistivity at this critical thickness, we compare a theoretical model of resistivity with our data. One model of resistivity in ultra-thin films assumes a homogenous and uniformly thick film (2). As the thickness is decreased, collisions with the surface begin to comprise a significant fraction of the total number of collisions. Of the surface collisions, it is those that are diffuse rather than specular that lead to resistivity. Figure 3 illustrates the difference between diffuse and specular scattering. An electron scattered diffusely has an equal probability of rebounding in any particular direction, regardless of its initial direction. In specular scattering, the electron collides elastically with the surface, thus producing no net change in velocity in the direction of the electron current density  $\bar{J}$ , and therefore does not increase the resistivity over the bulk value.

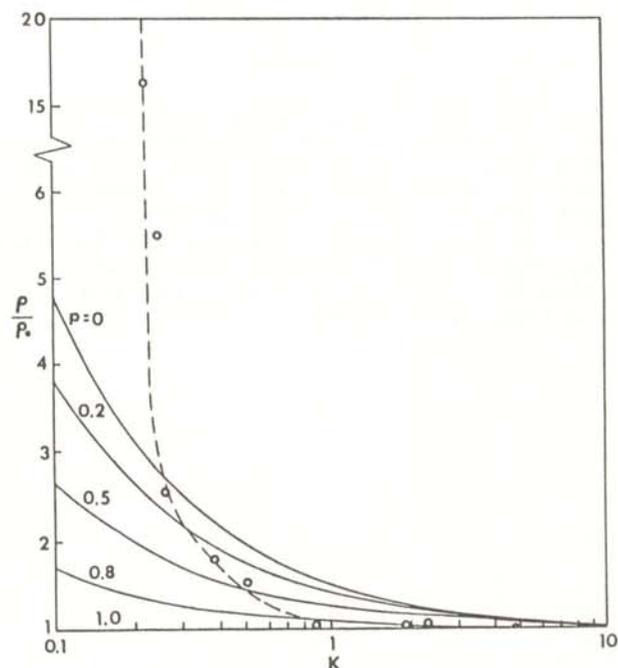


Figure 4  
Ratio of the film resistivity to bulk resistivity as a function of the ratio of film thickness to mean-free-path. The solid lines represent the values as computed by Campbell (2) for various probabilities of specular scattering. The dashed line represents our data.

Figure 4 compares theoretical plots of  $\rho/\rho_0$  versus  $K$ , the ratio of film thickness to mean-free-path, for various probabilities of specular scattering (2) with our data. We postulate that the inconsistency of the model is due to island formation (nucleation). As the film thickness is decreased, the film starts to become a collection of metal "islands" rather than one continuous piece of metal. When a film is evaporated, the metal atoms initially tend to agglomerate into islands analogous to the way water beads up on a freshly waxed car. The effect of nucleation is to restrict electron flow to the narrow contact bridges between islands, resulting in a very large resistivities.

Thin film nucleation is very common in some metals for thicknesses from 3 nm to 50 nm (3). In some cases, the resistivity of a metal does depend on the dimensions of the metal. Nucleation may be a limiting factor that should be considered when designing modernelectronic devices with sub-micron dimensions.

#### ACKNOWLEDGMENTS

The authors would like to thank John Zasadzinski for his support and guidance during this project. We would also like to thank Robert Zechman for the use of his scanning electron microscope, Rick Pastor for the valuable reference which he brought to our attention, and John Chrzas for his helpful suggestions.

#### REFERENCES

- (\*) This work was partially supported by an Allied-Bendix Award administered by the Society of Physics Students.
- (1) M. Ali Omar, Elementary Solid State Physics, Addison-Wesley, Reading, MA 1975.
- (2) L.I. Maissel, Handbook of Thin Film Technology, McGraw-Hill, New York, 1970.
- (3) R.S. Sennett and G.D. Scott, Journal of the Optical Society of America, 40,4, 1950, pp 203 - 211.

#### FACULTY SPONSOR OF THIS PAPER

Dr. John F. Zasadzinski  
Physics Department  
Illinois Institute of Technology  
Chicago, IL 60616